

# The preparation and thermoelectric properties of molten salt electrodeposited boron wafers

Y. Kumashiro,<sup>a,\*</sup> S. Ozaki,<sup>a</sup> K. Sato,<sup>a</sup> Y. Kataoka,<sup>a</sup> K. Hirata,<sup>a</sup> T. Yokoyama,<sup>a</sup>  
S. Nagatani,<sup>b</sup> and K. Kajiyama<sup>b</sup>

<sup>a</sup> Graduate School of Engineering, Yokohama National University, 79-5 Tokiwadai, Hodogaya-ku, Yokohama 240-8501, Japan

<sup>b</sup> MAC Science Company Ltd., 5289 Nagatsuda-cho, Midori-ku, Yokohama 226-0026, Japan

Received 27 September 2002; received in revised form 7 May 2003; accepted 16 May 2003

## Abstract

We have prepared electrodeposited boron wafer by molten salts with  $\text{KBF}_4\text{-KF}$  at  $680^\circ\text{C}$  using graphite crucible for anode and silicon wafer and nickel plate for cathodes. Experiments were performed by various molar ratios  $\text{KBF}_4/\text{KF}$  and current densities. Amorphous p-type boron wafers with purity 87% was deposited on nickel plate for 1 h. Thermal diffusivity by ring-flash method and heat capacity by DSC method produced thermal conductivity showing amorphous behavior in the entire temperature range. The systematical results on thermoelectric properties were obtained for the wafers prepared with  $\text{KBF}_4\text{-KF}$  (66–34 mol%) under various current densities in the range  $1\text{--}2\text{ A/cm}^2$ . The temperature dependencies of electrical conductivity showed thermal activated type with activation energy of 0.5 eV. Thermoelectric power tended to increase with increasing temperature up to high temperatures with high values of (1–10) mV/K. Thermoelectric figure-of-merit was  $10^{-4}/\text{K}$  at high temperatures. Estimated efficiency of thermoelectric energy conversion would be calculated to be 4–5%.

© 2003 Elsevier Inc. All rights reserved.

**Keywords:** Molten salt electrodeposition; Amorphous boron wafer; Electrical conductivity; Thermoelectric power; Thermal conductivity; Thermoelectric figure of merit

## 1. Introduction

Boron has a high melting point, high hardness and high thermoelectric power with a wide gap, which would be expected in thermoelectric materials used as a refractory semiconductor [1,2]. We prepared a boron film by the CVD process [3,4] and molecular beam deposition [5] utilizing dangerous diborane gases. Especially boron films prepared by molecular beam deposition showed very high electrical resistivity to the measurement of electrical properties by the van der Pauw method, which yielded low thermoelectric figure-of-merit values [6].

On the contrary, electrolysis process using powders as raw materials is inherently inexpensive and yield large area specimens. The major problem facing in molten salt experiment is the choice of a suitable solute and solvent system where stability at the deposition temperature is an important requirement [7]. The solvent should have a

high solubility, low viscosity, low melting point, low reactivity with container and electrode. It should be non-toxic and available in high purity at low cost. A review was given for electrodeposition of various semiconductors such as Si, Se, and compound semiconductor from molten salts [7]. As for boron, there are only limited data by patent [8,9], using  $\text{B}_2\text{O}_3\text{-KBF}_4\text{-KF}$  systems. The possibility of deposition of boron was studied in the molten salt containing 17 mol% of NaF and variable amounts of  $\text{KBF}_4$  [10]. There are only limited data by patent [8,9], using  $\text{B}_2\text{O}_3\text{-KBF}_4\text{-KF}$  systems.

We have prepared the electrodeposited boron wafers by molten salts with  $\text{KBF}_4\text{-KF}$  under various conditions and have measured electrical, thermal and thermoelectric properties to evaluate thermoelectric figure-of-merit.

## 2. Experimental

The experimental apparatus for the electrodeposition consists of graphite crucible (26 mm in inner diameter,

\*Corresponding author. Fax: +81-45-339-3949.

E-mail address: [kumasiro@ynu.ac.jp](mailto:kumasiro@ynu.ac.jp) (Y. Kumashiro).

30 mm in outer diameter, 28 mm in depth) for anode and silicon wafer ( $8 \times 1 \times 0.06 \text{ cm}^3$ ) and nickel plate ( $8 \times 1 \times 0.1 \text{ cm}^3$ ) for cathodes. The melt  $\text{KBF}_4$  (98% in purity) and  $\text{KF}$  (99% in purity) were contained in a graphite crucible within an argon (research grade) atmosphere maintained within the furnace. During each experimental run, argon was kept flowing through the chamber. After the  $\text{KBF}_4/\text{KF}$  mixtures were melted at  $680^\circ\text{C}$  by resistance heating, boron was deposited on cathode for 0.5–1 h under various current densities. DC current was supplied through a silicon rectifier. DC current and voltage were 1 A, and 15–30 V, respectively.

The quality of the specimen was evaluated by X-ray diffraction and SEM observation. The wafers were obtained by separating from nickel plate. The purities of the wafers were determined by X-ray photoelectron spectroscopy (XPS).

Ohmic contacts of the wafers were made by evaporated Al, followed by annealing in argon at  $400^\circ\text{C}$  for 1 h. Electrical properties of the wafer at room temperature were measured by the van der Pauw method. Electrical properties of the wafers were measured by a two-terminal method at temperature between room temperature and  $800^\circ\text{C}$  under argon atmosphere [3]. Thermoelectric voltage between hot and cold junctions was measured under a constant temperature gradient of  $2\text{--}3^\circ\text{C}$ . The specific heat capacity was measured on small wafers by DSC method in the temperature range  $60\text{--}500^\circ\text{C}$ . Thermal diffusivity of wafer was measured by the laser-flash method using a ring flash light [11]. Thermal conductivity was calculated from the measurement of thermal diffusivity and heat capacity.

### 3. Results and discussion

#### 3.1. Preparation of wafers

$\text{KF}$  would act to undergo high thermal decomposition at the bath temperature and  $\text{KBF}_4$  is boron source and is protected from thermal decomposition by being dissolved in  $\text{KF}$ . In the presence of an excess of fluoride ion, boron ions become fluoride. The boron would be directly produced in a one-step reaction by electro-reduction in fused  $\text{KF}$ .

The crystallinity of the boron film on Si (100) plane depends on molar ratios of  $\text{KBF}_4/\text{KF}$  and current densities. The films grown by  $\text{KBF}_4\text{--KF}$  (50–50 mol%) at current densities of  $100 \text{ mA/cm}^2$  contain mainly tetragonal (201), (103) and (331) planes with other small rhombohedral boron while decreasing of the ratio from 2 to 1 the film contains much rhombohedral boron peaks. Change in the composition from  $\text{KBF}_4\text{--KF}$  (50–50 mol%) to  $\text{KBF}_4\text{--KF}$  (66–34 mol%) produces amorphous structure. At current densities 33 and  $50 \text{ mA/cm}^2$ ,

the film did not show crystalline peak indicating amorphous structure is independent of the molar ratios. After the electrodeposition for 1 h boron deposited on Ni substrate was pulled upward from the melt in the crucible and was cooled down to room temperature. The deposited boron on the substrate was dipped into pure water in order to take away a residue of the melt. Then the boron wafer was peeled from the substrate by driving a pincette between wafer and substrate. Current efficiency of 10–14% was obtained, which would be due to the concentration motion of low valence ions from cathode to anode [12]. Current efficiency means the efficiency of deposition, which would be accompanied by simultaneous gas evolution. Total current efficiency represents the fraction of the total number of coulombs involved in the process. Low current efficiency in the present experiment brings about more faradays reaction at an electrode including side reactions, i.e., reduction or oxidation of solvent, supporting electrolyte, electrode materials or impurity. Furthermore, semiconducting Si wafer prevented long time growth experiment due to high resistivity, i.e.  $1 \Omega \text{ cm}$ , so we could not prepare boron wafer to measure thermoelectric properties.

Replacement of Si wafer by Ni plate resulted in a large current density above  $1 \text{ A/cm}^2$  to prepare wafers because Ni is metallic conductor to prepare wafers. After the electrodeposition for 1 h boron deposited on Ni substrate was pulled upward from the melt in the crucible and was cooled down to room temperature. The deposited boron on the substrate was dipped into pure water to take away a residue of the melt. Then the boron wafer was peeled from the substrate by driving a pincette between wafer and substrate. Fig. 1 shows SEM observation of the wafers. The wafer prepared by  $\text{KBF}_4\text{--KF}$  (50–50 mol%) has irregular surface and large grain, while that by  $\text{KBF}_4\text{--KF}$  (66–34 mol%) has comparatively fine grain with smooth surface.

Purity of the boron wafer electrodeposited on Ni plate is shown in Table 1 with  $\text{KBF}_4/\text{KF}$  ratios by chemical analysis and electrical properties. The formation of Ni–B compound was not detected. They are all p-type conductors. We could not measure Hall effect for the wafer prepared with  $\text{KBF}_4\text{--KF}$  (25–75 mol%) because of insufficient ohmic contact. Then we prepared wafers by  $\text{KBF}_4\text{--BF}$  (66–34 mol%). Current density dependences of electrical properties of the wafers are shown in Fig. 2. In increasing current density ( $J$ ), hole mobility ( $\mu$ ) decreases but electrical resistivity ( $\rho$ ) tends to saturate at  $2 \text{ A/cm}^2$ . Hole concentration ( $p$ ) increases in increasing current density and becomes maximum at  $2 \text{ A/cm}^2$  and then decreases at  $2.5 \text{ A/cm}^2$ . Low hole concentration of  $10^{13}\text{--}10^{14}/\text{cm}^3$  indicates that high density of intrinsic acceptor is compensated by oxygen and fluorine.

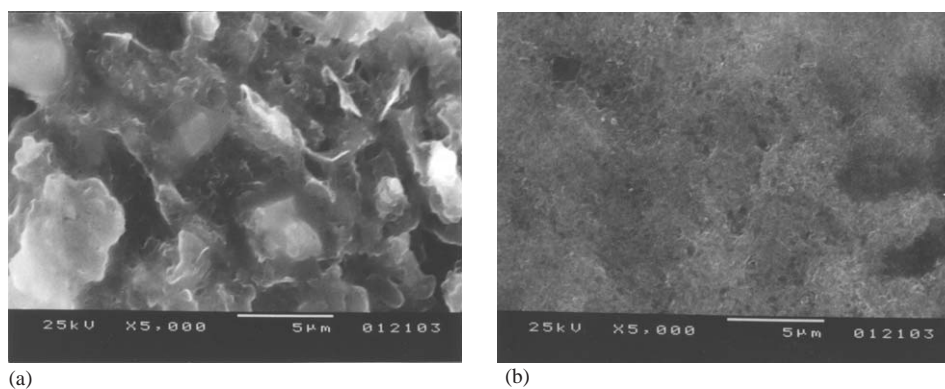


Fig. 1. SEM observation of the boron wafers. (A)  $\text{KBF}_4:\text{KF} = 1:1$  (B)  $\text{KBF}_4:\text{KF} = 2:1$ .

Table 1

Electrical properties of boron wafers together with the results by chemical analysis

$\text{KBF}_4:\text{KF}$ (molar ratio)	Hole concentration ( $\text{cm}^{-3}$ )	Mobility ( $\text{cm}^2/\text{V}\cdot\text{s}$ )	Resistivity ( $\Omega\cdot\text{cm}$ )	Chemical analysis for wafer (at%)
2:1	$1.2 \times 10^{14}$	19	$2.8 \times 10^3$	B: 87.6, C: 6.2, O: 6, K: 0.1, F: 0.1
1:1	$6.6 \times 10^{13}$	15	$6.3 \times 10^3$	B: 79.5, C: 11, O: 9, K: 0.3, F: 0.2

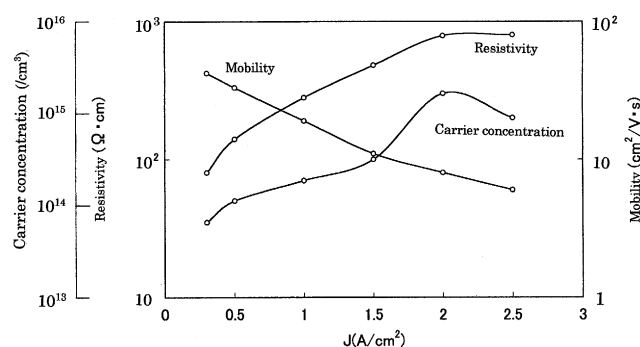


Fig. 2. Current density dependence of electrical properties.

### 3.2. Thermoelectric properties

Temperature dependencies of heat capacity ( $C_P$ ) are shown in Fig. 3, which give the Debye temperature ( $\theta$ ). The data include that of CVD amorphous wafer [3] as a standard. The present heat capacity at 340 K is 2.908 cal/mol K for CVD wafer, 2.734 and 2.783 cal/mol K for electrodeposited wafers. That for CVD wafer is in good agreement with cited value of 2.897 cal/mol K at room temperature [13], while those for electrodeposited ones deviate from the cited value owing to the impurities of the wafer. The heat capacity for CVD wafer shows gradual increase with increase in temperature, which is the usual behavior. Deviation of heat capacity of the electrodeposited wafers from that of CVD wafer and differences in the heat capacity between two electrodeposited wafers become large with increase in temperature. Minimum or maximum value around 700 K is observed, which would be due to the purities of the wafers (Table 1).

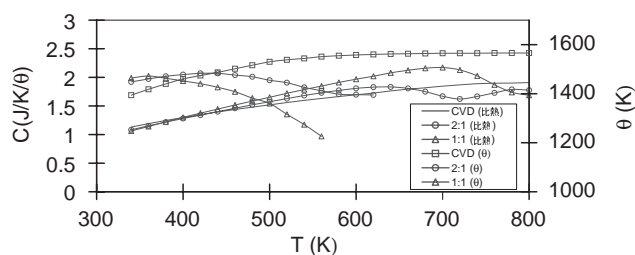


Fig. 3. Temperature dependence of heat capacity and Debye temperature. (The results of amorphous CVD wafer [3] is also shown.)

The value of  $\theta$  is obtained from specific heat at constant volume  $C_V$ , which is deduced with the usual thermodynamic formula

$$C_V = C_P - (\beta^2 V)/KT, \quad (1)$$

where  $\beta$  is the volume expansivity ( $\beta = 3\alpha$ , where  $\alpha$  is linear expansivity),  $K$  the isothermal compressibility and  $V$  the molar volume. There are no data on  $\alpha$  and  $K$  for amorphous boron. The narrow range and the range orders of a-B are closely related to those of  $\beta$ -B [2]. Then the data for  $\beta$ -B [14,15] were used with the value of  $V = 4.59 \text{ cm}^3$  and the published data for  $\alpha$  [15].  $C_P$  (Fig. 2) is converted to  $C_V$ . Then  $\theta$  is calculated with the formula

$$C_v/3R = (3/x) \int_0^{f_0} [x^4 e^x / (e^x - 1)^2] dx \quad (2)$$

with  $x = \theta/T$ ,

where  $R$  is the gas constant of 1.987 cal/mol K. The values of the right-hand term in Eq. (2) have been tabulated [16]. The temperature dependence of  $\theta$  is also shown in Fig. 3. The data for CVD amorphous wafer [2] are higher than those for  $\beta$ -B, which would be due to the

uncertainty of the parameter used. The Debye temperature and its temperature dependence for the CVD boron wafer would be reasonable and typical of the results for amorphous boron: a high Debye temperature reflects the low atomic mass and strong interatomic bonding in a-B, where external bonds of icosahedra in amorphous are largely covalently saturated [2].

On the contrary the present electrodeposited wafers are different from the CVD boron wafer. Decreases in  $\theta$  with increase in temperature are characteristic ones. Especially this is remarkable for the electrodeposited wafer with  $\text{KBF}_4\text{-KF}$  (50–50 mol%). The decreases in  $\theta$  would reflect a weak bonding due to formation of boron oxides, i.e.,  $\text{B}_2\text{O}_3$ ,  $\theta = 259 \text{ K}$  [17].

The temperature dependence of thermal conductivity, calculated as the product of specific heat capacity (Fig. 3), the thermal diffusivity (Fig. 4) and density  $2.354 \text{ g/cm}^3$  [19], is also shown in Fig. 4. The results are compared with that for CVD amorphous wafer [3], where the thermal conductivity is constant in a wide temperature range, showing characteristics of a glass as confirmed by Golikova et al. [18]. Our previous thermal conductivity for amorphous CVD boron wafer was calculated by using the reported heat capacity data [13], so that the present data would be more reasonable than the previous one [3]. The electrodeposited wafer prepared with  $\text{KBF}_4\text{-KF}$  (66–34 mol%) has lower thermal diffusivity and thermal conductivity than those of films prepared by amorphous CVD one, but temperature dependencies are similar to that of films prepared by CVD characterized by amorphous behavior. Initially the thermal conductivity increases as the specific heat increases. The comparatively low thermal conductivity increasing with increasing temperature is typical of a disordered or amorphous solid where the phonon mean free path is of the order of the interatomic spacing and independent of temperature [20].

The behavior in the electrodeposited wafer with  $\text{KBF}_4\text{-KF}$  (50–50 mol%) differs greatly from them with discrete maximum and rapid decrease in the thermal conductivity, which would depend on the purity and inhomogeneity in the wafer. Then this wafer would not be preferable to measure thermoelectric properties.

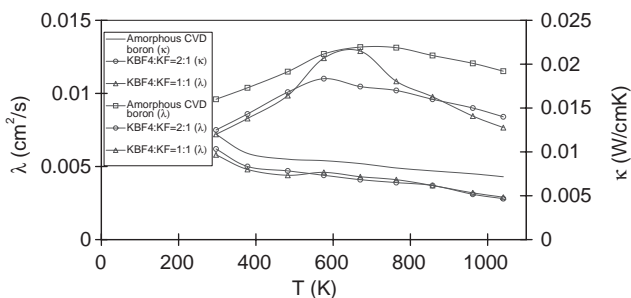


Fig. 4. Temperature dependence of thermal diffusivity and thermal conductivity. (The results of amorphous CVD wafer [3] is also shown.)

Temperature dependencies of electrical conductivities prepared at various  $\text{KBF}_4/\text{KF}$  ratios showed linear relationship between conductivities and reciprocal temperature with activation energies of 0.2–0.5 eV. However, their thermoelectric powers have large values of  $\sim 1 \text{ mV/K}$  but data scattered. No systematic behavior including thermoelectric figure-of-merit with respect to the ratio of  $\text{KBF}_4/\text{KF}$  was observed, except for  $\text{KBF}_4\text{-KF}$  (66–34 mol%), which would be due to inhomogeneity of the wafer reflected temperature dependencies of heat capacity and Debye temperature (Fig. 3).

Then thermoelectric properties of amorphous-boron wafer using  $\text{KBF}_4\text{-KF}$  (66–34 mol%) at various current densities were examined. Fig. 5 shows temperature dependencies of electrical conductivities as a function of current density. No appreciable difference is observed between them with activation energies of 0.5 eV, being nearly to absorption edge of about 0.7 eV [2]. These behaviors would be explained by almost same impurities states in the wafers. Fig. 6 shows temperature dependencies of thermoelectric powers as a function of current density. The thermoelectric power increases with increase in temperature up to about 600 K and becomes almost a constant or slightly decreases above 600 K. An increase of thermoelectric power would be explained by an additional term representing the entropy associated with the transport of vibrational energy with carrier [21]. Above 600 K, it tends to saturate, being similar to amorphous CVD wafer [3]. Thermoelectric power

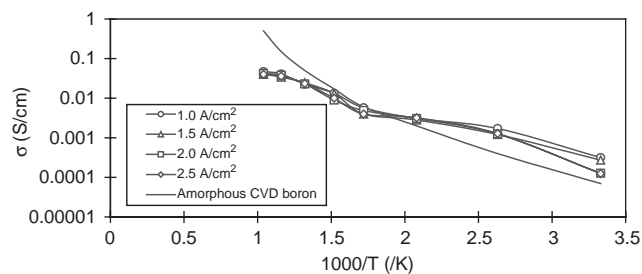


Fig. 5. Temperature dependence of electrical conductivity of boron wafer. (The results of amorphous CVD wafer [3] is also shown.)

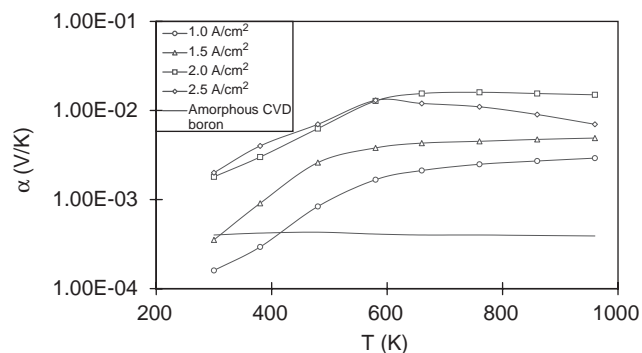


Fig. 6. Temperature dependence of thermoelectric power of boron wafer. (The results of amorphous CVD wafer [3] is also shown.)

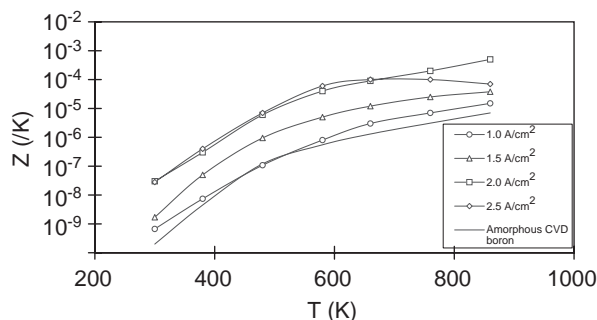


Fig. 7. Temperature dependence of thermoelectric figure of merit of boron wafer. (The results of amorphous CVD wafer [3] is also shown.)

increases with increase in current density at a fixed temperature and large values of 1–10 mV/K above 600 K should be noted. In the present current density, the discharge of ions occurs on the cathode rapidly so that growth rate becomes larger. Rapid growth in the wafer in increasing current density would be expected to introduce structural disorder (Fig. 2) although the differences of these wafers in the XRD pattern and SEM observation are not found.

The figure-of-merit ( $Z$ ) is calculated by thermoelectric power, electrical conductivity and thermal conductivity. Fig. 7 shows temperature dependencies of  $Z$  as a function of current density. The  $Z$  value increases with the increase in temperature. High thermoelectric power and low thermal conductivity contribute high  $Z$  but low mobility leads to strong decrease in  $Z$ . This would be due to microstructure in the wafer.  $Z$ -value for the wafer prepared by current density of 2 A/cm<sup>2</sup> should be noted at high temperatures.

The efficiency of thermoelectric devices with a hot ( $T_h$ ) and cold ( $T_c$ ) junction [22] would be estimated by theoretical efficiency of a Carnot machine and transport properties of  $Z$  on the condition that n- and p-types semiconductors of otherwise equal properties are available. When the efficiency of thermoelectric energy conversion would be estimated by  $T_h = 1500^\circ\text{C}$ ,  $T_c = 1000^\circ\text{C}$  and  $Z = 5.0 \times 10^{-4}/\text{K}$  a value of 4–5% could be obtained although n-type boron wafer with otherwise similar properties is not obtained. The present efficiency estimated is smaller than that for boron carbide of about 25% with some optimistic assumptions [22].

#### 4. Conclusion

We have succeeded in preparing amorphous p-type boron wafers by electrodeposition using  $\text{KBF}_4\text{-KF}$  (66–34 mol%) on nickel plate with various current densities (1–2.5 A/cm<sup>2</sup>) to measure thermoelectric prop-

erties. The wafers prepared at 2 A/cm<sup>2</sup> have the best results with  $Z$  value of  $5 \times 10^{-4}/\text{K}$  and efficiency of 4–6% where low thermal conductivity and high thermoelectric power contribute high  $Z$ , while low mobility leads to the strong decrease in  $Z$ . Optimum composition of the wafer would be expected to produce high  $Z$  and high efficiency.

#### Acknowledgments

This work was supported by Foundation of Promotion of Material Science and Technology of Japan (MST Foundation).

#### References

- [1] Y. Kumashiro, in: Y. Kumashiro (Ed.), *Electric Refractory Materials*, Dekker, New York, 2000, p. 557, p. 655.
- [2] H. Werheit, in: Y. Kumashiro (Ed.), *Electric Refractory Materials*, Dekker, New York, 2000, p. 589.
- [3] Y. Kumashiro, T. Yokoyama, K. Sato, Y. Ando, *J. Solid State Chem.* 133 (1997) 314–321.
- [4] Y. Kumashiro, K. Sato, S. Chiba, S. Yamada, D. Tanaka, K. Hyodo, T. Yokoyama, K. Hirata, *J. Solid State Chem.* 154 (2000) 39–44.
- [5] Y. Kumashiro, T. Yokoyama, T. Sakamoto, T. Fujita, *J. Solid State Chem.* 133 (1997) 269–272.
- [6] Y. Kumashiro, K. Hirata, K. Sato, T. Yokoyama, T. Aisu, T. Ikeda, M. Minaguchi, *J. Solid State Chem.* 154 (2000) 26–32.
- [7] D. Elwell, *J. Cryst. Growth* 52 (1981) 741–752.
- [8] H.S. Coopen, U.S. Patent 2572248, 2572249, 1951.
- [9] W.M. Weil, British Patent 677392, 684572, 1952.
- [10] F. Lantelme, A. Barhoun, M. Chemle, J. von Barner, *Electrochem. Soc. Proc.* 99-41 (2000) 612–623.
- [11] Y. Kumashiro, T. Mitsuhashi, S. Okaya, F. Muta, T. Koshiro, Y. Takahashi, M. Hirabayashi, *J. Appl. Phys.* 65 (1989) 2147–2148.
- [12] M. Maja, N. Penajji, M.V. Ginatta, G.M. Orsello, *J. Electrochem. Soc.* 137 (1990) 3498–3504.
- [13] S.S. Wise, J.L. Margrave, R.L. Altman, *J. Phys. Chem.* 64 (1960) 915–917.
- [14] C.E. Holcombe, D.D. Smith, J.D. Lord, W.K. Diereses, D.A. Carpenter, *High Temp. Sci.* 5 (1973) 349–357.
- [15] J.G. Bower, in: Brotherton, Steinberg (Eds.), *Progress in Boron Chemistry*, Pergamon Press, Oxford, 1970, p. 231.
- [16] E.S.R. Gopal, in: *Specific Heats at Low Temperature*, Plenum, New York, 1966, p. 221.
- [17] G.K. White, S.J. Collocott, J.S. Cook, *Phys. Rev. B* 29 (1984) 4778–4781.
- [18] O.A. Golikova, A. Tadghiev, *J. Non-Cryst. Solids* 87 (1986) 64–69.
- [19] C.P. Talley, L.E. Line, Q.D. Overman Jr., in: J.A. Kohn, W.F. Nye, G.K. Gaulé (Eds.), *Boron*, Vol. 1, Plenum Press, New York, 1960, p. 94.
- [20] J.E. Parrott, A.D. Stuckes (Eds.), *Thermal Conductivity of Solids*, Pion, London, 1975, p. 90.
- [21] T.L. Aselage, *Mater. Res. Soc. Symp. Proc.* 234 (1991) 145–156.
- [22] H. Werheit, *Mater. Sci. Eng. B* 29 (1995) 228–232.